



Title	Effect of temperature on the aggregation of an Fc-fusion protein under agitation
Author(s)	Wang, Zekun; Gambe-Gilbuena, Arni; Unzai, Satoru et al.
Citation	European Journal of Pharmaceutical Sciences. 2025, 215, p. 107320
Version Type	VoR
URL	https://hdl.handle.net/11094/103669
rights	This article is licensed under a Creative Commons Attribution 4.0 International License.
Note	

The University of Osaka Institutional Knowledge Archive : OUKA

<https://ir.library.osaka-u.ac.jp/>

The University of Osaka



Effect of temperature on the aggregation of an Fc-fusion protein under agitation

Zekun Wang ^a , Arni Gambe-Gilbuena ^b, Satoru Unzai ^c, Susumu Uchiyama ^{a,d,*}, Tetsuo Torisu ^{a,*} 

^a Department of Biotechnology, Graduate School of Engineering, The University of Osaka, 2-1 Yamadaoka, Suita, Osaka 565-0871, Japan

^b U-Medico Inc., 2-1 Yamadaoka, Suita, Osaka 565-0871, Japan

^c Nihon Waters K.K., No5. Koike Bldg, 1-3-12 Kita-Shinagawa, Shinagawa-ku, Tokyo 140-0001, Japan

^d Exploratory Research Center on Life and Living Systems, National Institutes of Natural Sciences, 5-1 Higashiyama, Myodaiji, Okazaki, Aichi 444-8787, Japan



ARTICLE INFO

Keywords:

Protein stability
Protein aggregation
Fc-fusion protein
Agitation stress
Thermal stress

ABSTRACT

Mitigating protein aggregation remains a challenge in the development of biopharmaceuticals, and agitation is well known as a stress that can induce protein aggregation. However, the temperature dependence of agitation-induced aggregation is not well understood. In this study, the aggregation of an Fc-fusion protein under agitation stress was investigated at 5, 25, and 40 °C. Soluble and insoluble aggregates were quantified by size-exclusion liquid chromatography and flow imaging microscopy, respectively. Both the aggregation level and the aggregate clusters were temperature dependent. The threshold for the orbital shaking that induced protein aggregation was temperature independent. Although thermal stress at 40 °C increased the number of oligomers, it did not lead to a higher monomer loss in a subsequent agitation at 25 °C. The aggregation induced by agitation stress was suppressed by adding a surfactant or removing the vial headspace, indicating that the aggregation occurred via an interface-mediated pathway. Thus, the observed temperature dependence was attributed to the protein adsorption to the interface and the following interfacial unfolding and aggregation was affected by the temperature. The results emphasized the importance of temperature control during shipping to ensure the quality of drug products. Agitation stability studies at a controlled temperature also provide a deep understanding of the protein aggregation mechanism, which is important for formulation development.

1. Introduction

Therapeutic proteins, including monoclonal antibodies and Fc-fusion proteins, have been developed rapidly in recent decades because of their successful use in treating various human diseases (Grilo and Mantalaris, 2019; Walsh, 2018). Fc-fusion proteins consist of an immunoglobulin Fc domain that is directly linked to a proteinaceous molecule of interest, such as a ligand or antigen, to expand the practicability of using the antibody (Czajkowsky et al., 2012). The structures of Fc-fusion proteins are easily disturbed, which can result in aggregation (Strand et al., 2013), leading to side effects in therapeutic proteins (Sperinde et al., 2020). Accordingly, therapeutic proteins, including Fc-fusion proteins, are often more sensitive to both internal and external stresses compared with small-molecule drugs. Because Fc-fusion proteins generally exhibit a lower conformational stability than monoclonal antibodies (Fast et al.,

2009), Fc-fusion proteins may be more susceptible to stress-induced degradation.

Protein aggregation is a physical degradation process inherent to proteins, which can be induced by various stresses to which therapeutic proteins may be exposed prior to administration. During aggregation, monomeric proteins associate to form larger aggregates, ranging in size from nanometers to micrometers, or even aggregates large enough to be visible (Amin et al., 2014; Carpenter et al., 2009; Roberts et al., 2011). These aggregates can trigger immunogenic responses and studies have suggested that the risk of immunogenicity depends on the size of the aggregates, although the particle size that induces the most immunogenicity is also protein dependent (Fathallah et al., 2015; Freitag et al., 2015; Kijanka et al., 2018; Krayukhina et al., 2019; Moussa et al., 2016; Rosenberg, 2006; Telikepalli et al., 2015). Previous studies have indicated that, in addition to insoluble aggregates, the formation of soluble

* Corresponding authors at: Department of Biotechnology, Graduate School of Engineering, The University of Osaka, 2-1 Yamadaoka, Suita, Osaka 565-0871, Japan.

E-mail addresses: suchi@bio.eng.osaka-u.ac.jp (S. Uchiyama), tetsuo.torisu@bio.eng.osaka-u.ac.jp (T. Torisu).

aggregates should be carefully controlled to avoid possible immunogenicity (Fathallah et al., 2015; Freitag et al., 2015; Kijanka et al., 2018). Therefore, it is essential to evaluate and understand the mechanisms behind the formation of the whole range of aggregates to minimize the formation and reduce unexpected risks associated with such aggregation.

Agitation stress is a common stress factor that can trigger protein aggregation. Proteins are frequently exposed to agitation stress during manufacture and transportation. We have recently reported that protein aggregation can be accelerated even by a weak vibration from the compressor of a refrigerator (Kizuki et al., 2025). Previous studies have shown that protein aggregation by agitation stress occurred via an interface-mediated pathway (Ghazvini et al., 2016; Grigolato and Arosio, 2020; Yoneda et al., 2021). Proteins tend to adsorb to interfaces because of their amphiphilic nature and undergo structural changes, making proteins prone to aggregation (Das et al., 2020; Li et al., 2019; Sreenivasan et al., 2021b; Toprakcioglu et al., 2022). The air-liquid interface is a key factor in the formation of protein aggregates via interface-mediated pathways (Kizuki et al., 2023). Several studies have shown that periodic changes in the surface area of the air-liquid interface, also referred to as compression and dilatation, played a critical role in aggregation via the air-liquid interface (Bee et al., 2012; Kiese et al., 2008; Koepf et al., 2018). Practically, removing or reducing the air-liquid interface by fully filling containers, or adding surfactants that prevent proteins from reaching the interface, can considerably suppress the formation of aggregates (Kiese et al., 2008; Kizuki et al., 2023; Li et al., 2019; Torisu et al., 2017).

Interfacial-induced aggregation has been reported to be temperature dependent; however, the mechanism of the combined effect of agitation and thermal stress on protein aggregation remains elusive. Wood et al. have shown that aggregate formation under interfacial stress was temperature dependent by periodically rotating vials horizontally and vertically. This temperature dependence was attributed to the coexistence of both bulk solution and interface-mediated aggregation pathways (Wood et al., 2020). Griffin et al. have also reported that such temperature dependence was observed in the aggregates generated under periodical interfacial compression and dilatation stresses provided by a Langmuir trough, but found that thermal stress enhanced the surface activity of the proteins (Griffin et al., 2022). We have recently reported that there was a threshold for the agitation conditions required to generate insoluble aggregates using a tri-axial vibrator, which causes harsher agitation compared with the shaker that is usually used for shaking stress studies (Kizuki et al., 2023). However, the threshold for the agitation conditions that cause aggregation using a shaker and the temperature dependence of the aggregation have not yet been investigated. Understanding the temperature dependence of agitation-induced aggregation is important to ensure the quality and safety of biopharmaceuticals prior to administration. During transportation, failure to control the temperature could expose biopharmaceuticals to combined thermal and agitation stress. In addition, during the handling process, even though liquid formulations of biopharmaceuticals are stored at 2–8 °C, restoration to ambient temperature is needed before compounding and administration, which is accompanied by manual handling during which thermal stress may also combine with agitation stress to contribute to protein aggregation (Cappelletto et al., 2024). In addition, consideration of the temperature dependence is important in the design of appropriate stress stability studies of agitation stress conducted during biopharmaceutical development.

The present study aimed to quantitatively analyze the interplay between thermal and agitation stresses on protein aggregation. We sought to elucidate whether these two stresses act independently, synergistically, or antagonistically, and to identify the temperature-dependent and -independent characteristics of agitation-induced aggregation. A fusion protein composed of a recombinant immunoglobulin G (IgG) Fc domain and the soluble part of the T-cell receptor (CTLA4-Ig) was placed in vials and exposed to both thermal and agitation stresses

simultaneously. Protein aggregates were analyzed using size-exclusion high-performance liquid chromatography (SE-HPLC) and flow imaging microscopy (FIM). In addition, the mechanism by which thermal stress accelerates particle formation is discussed, and the importance of temperature control in protein stability assessments is clarified.

2. Materials & methods

2.1. Materials

Butyl rubber stoppers and 2 mL borosilicate glass vials (16 × 33 mm) were purchased from Daiwa Special Glass Co., Ltd. (Osaka, Japan). Poloxamer 188 (Kolliphor® P 188 Bio) was a gift from BASF Japan (Tokyo, Japan). Unless otherwise specified, all other reagents were purchased from FUJIFILM Wako Pure Chemical Corporation (Osaka, Japan).

CTLA4-Ig was used as a model protein therapeutic that is sensitive to agitation stress (Kizuki et al., 2023). CTLA4-Ig was purchased from Ono Pharmaceutical Co., Ltd. (Osaka, Japan). To remove the surfactant in the commercial formulation, CTLA4-Ig was diluted with 10 mM sodium phosphate buffer (pH 7.0) and loaded onto a Q HP column (Cytiva, Buckinghamshire, UK) connected to an AKTA prime plus system (Cytiva). The protein was then eluted with 100 mM sodium phosphate buffer (pH 7.0) containing 400 mM NaCl. The eluted CTLA4-Ig solutions were further dialyzed against 10 mM sodium phosphate buffer (pH 6.0) using Slide-A-Lyzer G2 dialysis cassettes (10 K MWCO) (Thermo Fisher Scientific, Waltham, MA, USA). Dialyzed protein solutions were diluted to 1.0 mg/mL in the phosphate buffer and filtered through 0.22 μm polyethersulfone filters before experiments. Samples containing 0.8 % P188 were prepared by mixing the dialyzed protein solution with a phosphate buffer containing 1.6 % P188 in a 1:1 ratio, followed by concentration adjustment using a phosphate buffer with 0.8 % P188. A total of 1.5 mL of protein solution was filled into vials, which were washed three times with ultrapure (18.2 MΩ filtered) water and autoclaved prior to use, in a biological safety cabinet to ensure the absence of contamination.

2.2. Combination of thermal and agitation stress

The vials filled with CTLA4-Ig were placed horizontally on a BC-740 orbital shaker (BIO—CRAFT, Tokyo, Japan) to allow the solution to contact the rubber stopper and maximize the air-liquid interface in the vial, simulating the worst-case scenario of degradation caused by agitation stress (Kiese et al., 2008; Sreenivasan et al., 2021a; Wiesbauer et al., 2013). The shaker was used in an LHU-113 incubator (ESPEC Corp., Osaka, Japan) to subject the vials to agitation stress at the desired temperature. Vials placed on the shelf of the incubator horizontally were prepared as controls without agitation stress. The vials on the orbital shaker were subjected to 100 or 200 rpm agitation for up to 72 h, at temperatures of 5, 25, and 40 °C. Samples were taken at 0, 24, 48, and 72 h (and also at 0, 3, and 6 h for samples at 40 °C because of the high monomer loss over the first 24 h) after the start of agitation. Three vials were randomly selected from each group at each time point, and the contents of these three vials were mixed prior to analysis to obtain sufficient sample volume.

2.3. SE-HPLC

SE-HPLC was performed to quantify the amount of monomers and soluble aggregates in the samples. Samples were centrifuged at 15,000 rpm at 5 °C for 30 min using an Allegra X-30R centrifuge (Beckman Coulter, Pasadena, CA, USA) to avoid column clogging by insoluble aggregates. The supernatants were injected into an Acuity UPLC system (Waters, Milford, MA, USA) equipped with a TSKgel UP-SW3000 or TSKgel UP-SW3000LS column (4.6 × 150 mm; TOSOH, Tokyo, Japan) at room temperature. The sample injection volume was set to 20 μL.

Isocratic elution was performed for 11 min with a flow rate of 0.25 mL/min using 133 mM phosphate buffer containing 200 mM potassium chloride. UV absorbance at 280 nm was monitored for detection. Data were analyzed using Empower 3 Software (Waters). The percentages of the monomer and soluble protein (composed of monomer and oligomers eluted before the monomer) after stress tests in the total amount of protein were calculated by dividing the area of each peak by the areas at the initial time point.

2.4. FIM

A FlowCam 8100 (YOKOGAWA Fluid Imaging Technologies, Scarborough, ME, USA) equipped with an 80 μm flow cell and a 10 \times magnification lens was used to quantify the number concentration of subvisible particles larger than 2 μm (equivalent spherical diameter). A sample volume of 150 μL was analyzed at a flow rate of 0.05 mL/min for each measurement, with three measurements conducted for each condition. Data analysis was performed using VisualSpreadsheet software (YOKOGAWA Fluid Imaging Technologies). The particle identification settings were set to a 1 μm distance to the nearest neighbor, and the “close holes” parameter was set to 0. A particle segmentation threshold of 15.00 was applied for both dark and light pixels. Equivalent spherical diameter was used when evaluating the size of particles. Morphology was evaluated by both circularity and intensity (the relative brightness of each particle image).

2.5. Dynamic light scattering (DLS)

DLS measurements were conducted using a Zetasizer Ultra (Malvern Panalytical Ltd., Malvern, UK) to analyze submicron particles. The detection was performed using backscattering (174.4°). Samples were equilibrated at 25 °C for 120 s in quartz cuvettes with an optical path length of 3 \times 3 mm (Ultra-Micro cells, Hellma Analytics, Müllheim, Germany). For each sample, three consecutive measurements were taken. All other instrument settings were maintained at the default values recommended by the ZX Xplorer software (version 1.3.0.140).

2.6. Size exclusion chromatography with multi-angle laser light scattering (SEC-MALS)

SEC-MALS was performed to quantify the mass of aggregate clusters. The samples were injected into an Arc HPLC system (Waters Corporation) equipped with a XBridge Premier Protein SEC Column (250 Å, 2.5 μm , 7.8 \times 300 mm; Waters) at room temperature equipped sequentially with a DAWN™ MALS detector (Wyatt Technology, LLC) and Optilab™ refractive index (RI) detector (Wyatt). The sample injection volume was set to 25 μL . Isocratic elution was performed for 30 min with a flow rate of 0.5 mL/min using 133 mM phosphate buffer containing 200 mM potassium chloride. The MALS detector employed a laser source at 658 nm and 18 detectors at angles evenly positioned between 22.5° and 147°. RI detection was at 660 nm. Output signals from the MALS and RI detectors were imported into ASTRA™ software (Wyatt) for data processing.

2.7. Evaluation of synergistic effects

The synergistic effect of agitation and thermal stresses was evaluated using the synergistic effect and observed effect index equation [Eq. (1)] (González and Nazareno, 2011; Scmoroscenco et al., 2022; Yanwinitchai et al., 2024):

$$SE = \frac{\%OE}{\%TE} \quad (1)$$

where SE = synergistic effect, %OE = percentage of the observed effect of combined thermal and agitation stresses (experimental data), and %

TE = percentage of theoretical effect of combined thermal and agitation stresses [Eq.(2)]. The percentage of all sizes of protein aggregates based on the SE-HPLC data was used to calculate the observed effect under each type of stress.

The theoretical effect was calculated by summing the individual effects: agitation at 5 °C and thermal stresses without agitation. The intersected effect was then subtracted from this sum, according to the following equation (Yanwinitchai et al., 2024).

$$\%TE = \%OE_{\text{Thermal}} + \%OE_{\text{Agitation}} - \frac{(\%OE_{\text{Thermal}})(\%OE_{\text{Agitation}})}{100} \quad (2)$$

If the observed effect exceeds the theoretical effect, resulting in an SE greater than 1, a synergistic effect is deduced. An SE value of 1 indicates an additive effect, whereas SE < 1 denotes an antagonistic effect. Because the %TE should be a non-zero real number, the SE is considered positive infinity when the %TE is zero but the %OE is non-zero.

2.8. Pre-incubation at 40 °C before agitation stress at 25 °C

Samples were placed horizontally in plates within the incubator at 5 and 40 °C for 3 days without shaking. Immediately after the incubation, the samples were subjected to 200 rpm agitation stress for 72 h at 25 °C. Three vials were taken from each group at 0, 24, 48, and 72 h, and analyzed using SE-HPLC and FIM, as described above.

2.9. Far-UV circular dichroism (CD) spectroscopy

To evaluate the secondary structure of CTLA4-Ig monomer after the pre-incubation at 40 °C, the monomer was fractioned using a Prominence UFLC system (Shimadzu, Kyoto, Japan) equipped with a TSKgel UP-SW3000LS column (4.6 \times 150 mm; TOSOH, Tokyo, Japan), followed by buffer exchange into the phosphate buffer. CD spectra were obtained using a J-1500 CD spectropolarimeter (Jasco, Tokyo, Japan) equipped with a PM-539 detector. CD spectra of the samples were collected at a path length of 1 mm in the far UV region (190–280 nm) with a step size of 0.5 nm at 25 °C. The spectrum of the blank (10 mM sodium phosphate buffer, pH 6) was subtracted from the sample spectra. The observed ellipticity (θ_{obs}) in millidegrees was converted to mean residue ellipticity (MRE) in deg $\text{cm}^2 \text{dmol}^{-1}$, which was calculated from the equation:

$$MRE = \frac{\theta_{205} \times \varepsilon_{205}}{10 \times A_{205} \times n}$$

where n is the number of amino acid residues (358 for CTLA4-Ig) and ε_{205} is the extinction coefficient at 205 nm. The extinction coefficient of CTLA4-Ig was calculated as 1338,540 $\text{M}^{-1}\text{cm}^{-1}$ from the protein sequence using the Protein Parameter Calculator (Anthis and Clore, 2013). A_{205} is the absorbance at 205 nm measured using a J-1500 spectropolarimeter.

2.10. Differential scanning calorimetry (DSC)

The structural stability of CTLA4-Ig was evaluated using a MicroCal PEAQ-DSC automated system (Malvern Panalytical Ltd., Worcestershire, UK). The thermograms were acquired with a scanning rate of 60 °C/h, from 20 to 95 °C. A low level of feedback was employed and the progress method was used for baseline correction. The dialysis buffer was used as a reference. All DSC thermograms were corrected by subtracting the thermogram of the respective buffers and were analyzed using a non-two-state model in MicroCal PEAQ-DSC software V1.51.

2.11. Surface tension measurements

Dynamic surface tension was measured by the pendant drop method using a Theta Flex instrument (Biolin Scientific, Gothenburg, Sweden). In the measurements, a 10 μL pendant drop was generated at a flow rate

of 2 μ L/s, and the shape of the pendant drop was monitored for 300 s. The surface tension was simultaneously calculated from the Young–LaPlace equation every 10 s using OneAttension (ver.4.0.3).

2.12. Statistical analysis

The differences in particle levels between the initial time point and each subsequent time point were assessed using Dunnett's multiple comparison test. All statistical analyses were conducted using Python 3.9.6 with *scipy* and *statsmodels* packages for implementation of homogeneity of variance test, ANOVA analysis, and Dunnett's test.

3. Results and discussion

3.1. Protein aggregation under thermal stress

Prior to investigating the temperature dependence of CTLA4-Ig aggregation under agitation stress, the stability under thermal stress was evaluated. The stability of CTLA4-Ig at 5 and 25 °C, corresponding to storage in a refrigerator and at room temperature, respectively, were evaluated for up to 72 h. In addition, a stability study at 40 °C, a temperature slightly lower than the T_{onset} value of CTLA4-Ig based on the DSC results (Figure S1), was conducted. This temperature was selected

to assess the effect of temperature on agitation-induced aggregation with minimal contribution of heat-induced structural change and aggregation in bulk solution.

The monomer % value of CTLA4-Ig did not obviously decrease at 5 and 25 °C, whereas a rapid decrease in the monomer % was observed (Fig. 1a, b), and the peak derived from soluble oligomers was increased, at 40 °C (Fig. 1c). The total peak area was not decreased even at 40 °C for 72 h, indicating that most of the monomers lost under 40 °C conditions were converted to soluble aggregates. FIM showed that insoluble aggregates were significantly increased ($p < 0.05$) at 40 °C (Fig. 1d); however, the particle concentration was <1000 particles/mL and in the same order of magnitude as that before heating. Thus, this result also suggested that thermal stress at 40 °C mainly generated soluble oligomers from the monomers, and the generation of insoluble aggregates was limited.

The addition of 0.8 % P188 slightly suppressed the decrease in the monomer % at 40 °C (Fig. 1a, c). The total peak area was not decreased and no significant increase in the content of insoluble aggregates was observed in the presence of P188 (Fig. 1b, d). Although surfactants can prevent both bulk- and interface-mediated aggregation, a more prominent preventive effect toward interface-mediated aggregation than toward aggregation in bulk solution has been reported for polysorbate surfactants (Arsiccio and Pisano, 2018; Li and Roberts, 2010). Although

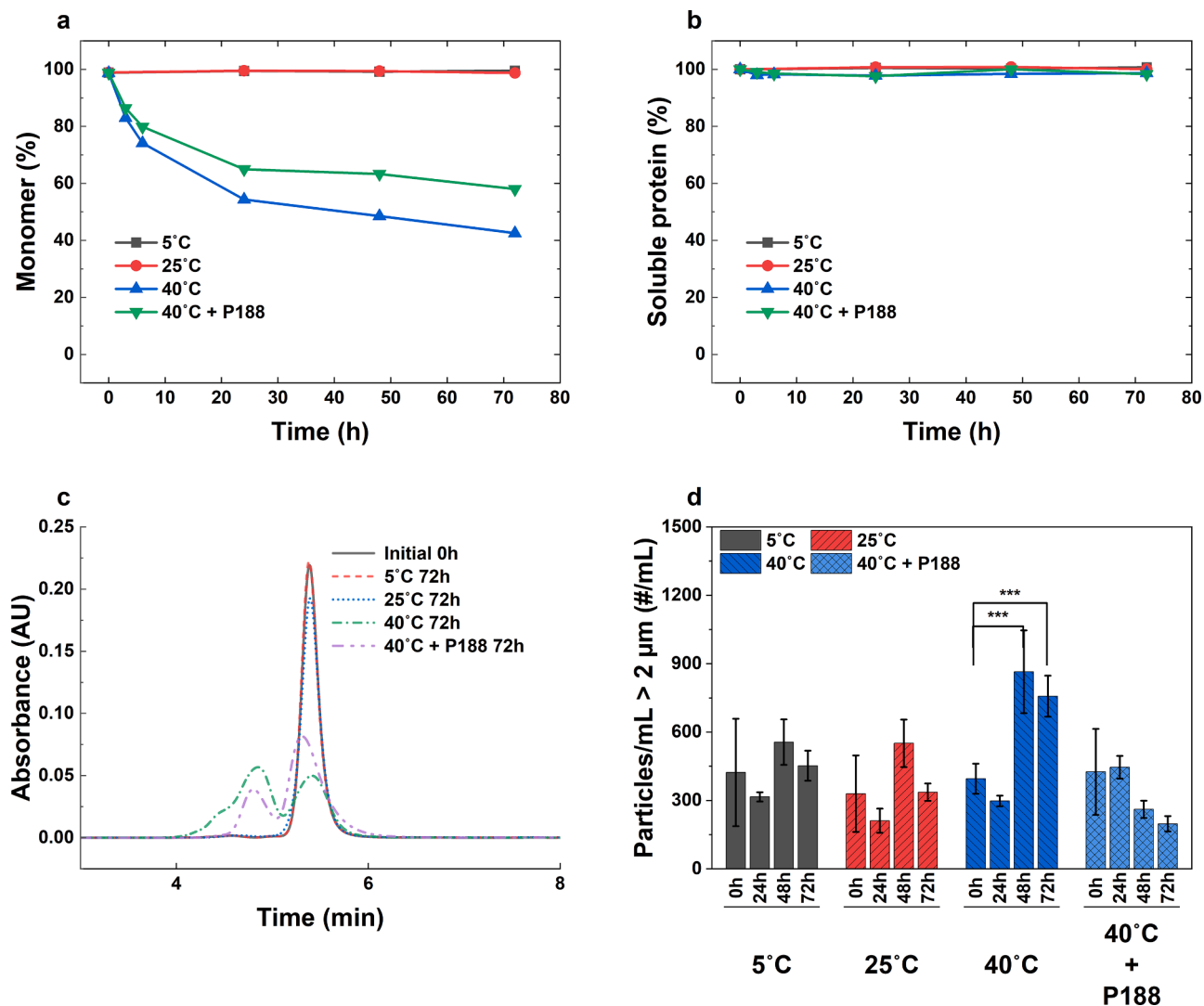


Fig. 1. Effect of thermal stress on the stability of 1.0 mg/mL CTLA4-Ig. (a) Monomer loss, (b) soluble protein loss, (c) corresponding SE-HPLC chromatograms, and (d) average particle count measured by FlowCAM at 5–40 °C, with and without P188.

P188 has lower surface activity than polysorbates (Li et al., 2024), P188 at 0.8 % is considered to exert a stabilizing effect against interface-mediated aggregation, comparable to that of polysorbates, by competitively occupying the interface (Bollenbach et al., 2022; Kizuki et al., 2023). Thus, the limited preventive effect of the surfactant on the aggregation induced by thermal stress inferred that thermal stress predominantly induces aggregation by the bulk solution pathway.

3.2. Protein aggregation by agitation stress without thermal stress

The amounts of both soluble oligomers and insoluble aggregates were not increased at 5 °C, and therefore agitation stress at three different frequencies (0, 100, and 200 rpm) was applied for 72 h at 5 °C to examine the aggregation induced by agitation stress alone. The monomer % value was not decreased at 0 or 100 rpm, whereas an obvious decrease in the monomer % was observed, and peaks that eluted between 3.4 and 4.8 min appeared, when the vials were shaken at 200 rpm (Fig. 2a). The total peak area was unchanged even by agitation at 200 rpm (Fig. 2b). An increase in the number of insoluble aggregate particles was observed, although the particle concentration was <1000 #/mL and in the same order of magnitude as that before agitation (Fig. 2d). Thus, as with the aggregation under thermal stress, most of the monomers lost by agitation at 200 rpm were likely to be converted to

soluble aggregates.

Interestingly, the elution times of the soluble oligomers were different between the conditions of thermal and agitation stress, and the soluble oligomers generated by the agitation stress had a shorter retention time. Samples incubated at 5 °C with agitation and incubated at 40 °C without agitation were analyzed by SEC-MALS to characterize the soluble oligomers. The molar mass of the two oligomers generated by thermal stress without agitation were 183.2 kDa (\pm 0.149 %) and 275.9 kDa (\pm 0.228 %), corresponding to a dimer and a trimer, respectively (Fig. 3a). In addition, minor components with molar masses of up to approximately 630 kDa (7-mers) were observed (Fig. 3a). Notably, under agitation stress at 5 °C, the peak eluting at approximately 11.5 min (the longest retention time within the oligomer fraction) corresponded to an oligomer with a molar mass of 198.4 kDa (\pm 0.238 %) and was considered a dimer (Fig. 3b), although the retention time was different to that of the dimer peak generated by thermal stress. This difference could be because the hydrodynamic radii of the dimers corresponding to the two peaks were different and suggests that the aggregation mechanisms of thermal stress and agitation stress may also be different. Moreover, no clear peak for a trimer was observed under agitation stress at 5 °C, while molar masses corresponding to tetramers were detected. This finding further supports the notion that the aggregation mechanism of thermal generated oligomers differs from that of

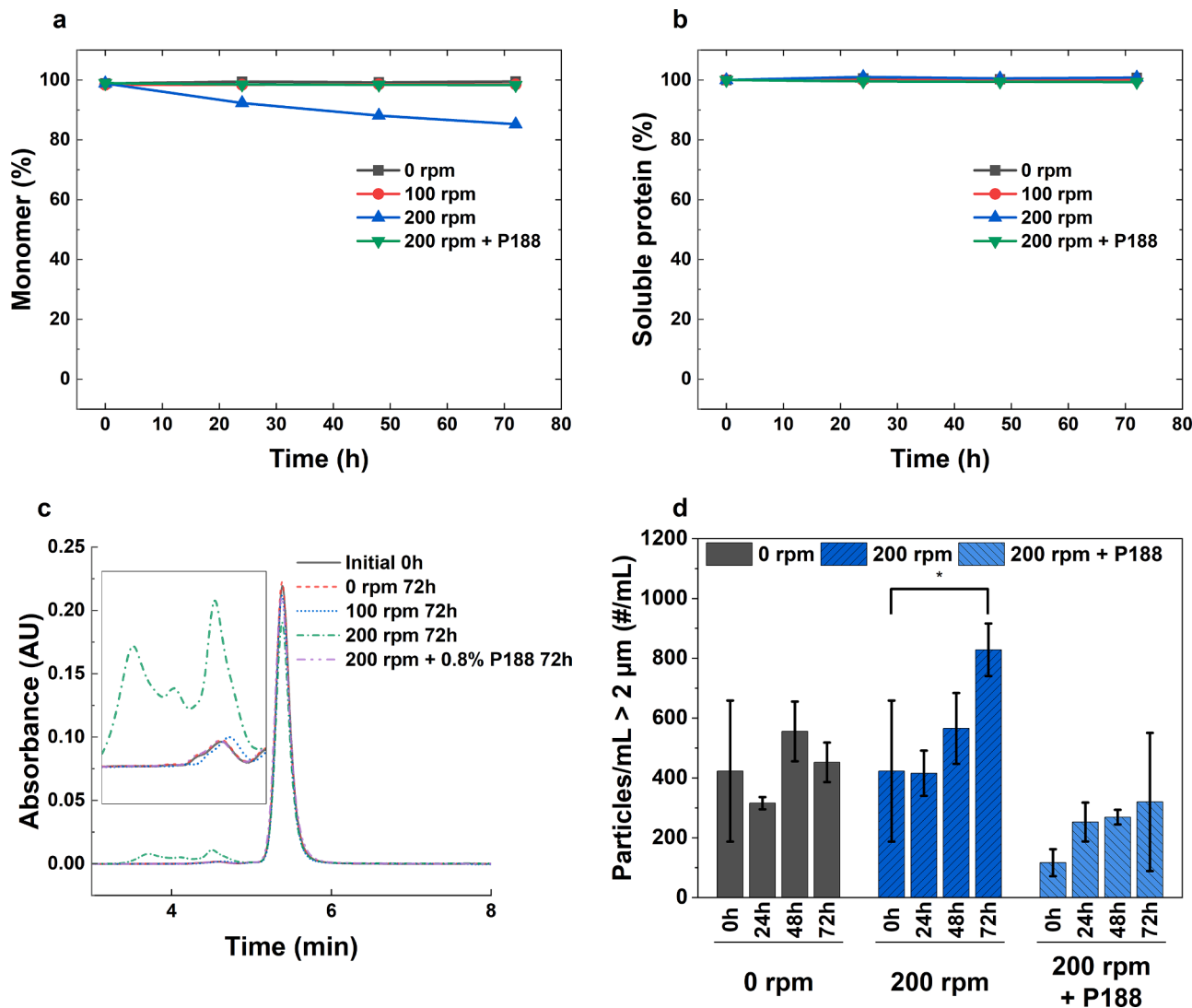


Fig. 2. Effect of agitation stress on the stability of 1.0 mg/mL CTLA4-Ig. (a) Monomer loss, (b) soluble protein loss, (c) corresponding SE-HPLC chromatograms, and (d) average particle count measured by FlowCAM under 0–200 rpm agitation, with and without P188.

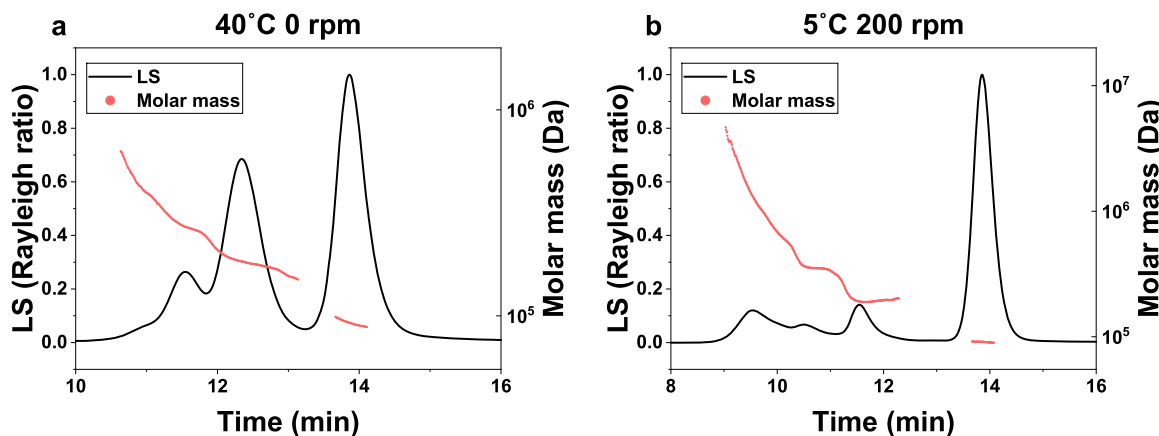


Fig. 3. SEC-MALS chromatogram of CTLA4-Ig under different stress conditions at 72 h. (a) At 40 °C without orbital shaking and (b) at 5 °C with 200 rpm orbital shaking.

oligomers generated by agitation stress. For simplicity, the oligomers generated by agitation stress are referred to here as early-eluting oligomers (EOO), whereas those generated by thermal stress are referred to as late-eluting oligomers (LEO).

In contrast to the aggregation under thermal stress at 40 °C, the decrease in monomer % value under agitation stress was totally prevented by the addition of P188 (Fig. 2a). The increase in insoluble

aggregates was also suppressed by the addition of P188. The differences in the oligomer profiles in SE-HPLC and the preventive effect of P188 suggested that thermal stress and agitation stress could have distinct mechanisms to cause protein aggregation, and the aggregation by agitation stress could be considered to occur via an interface-mediated pathway.

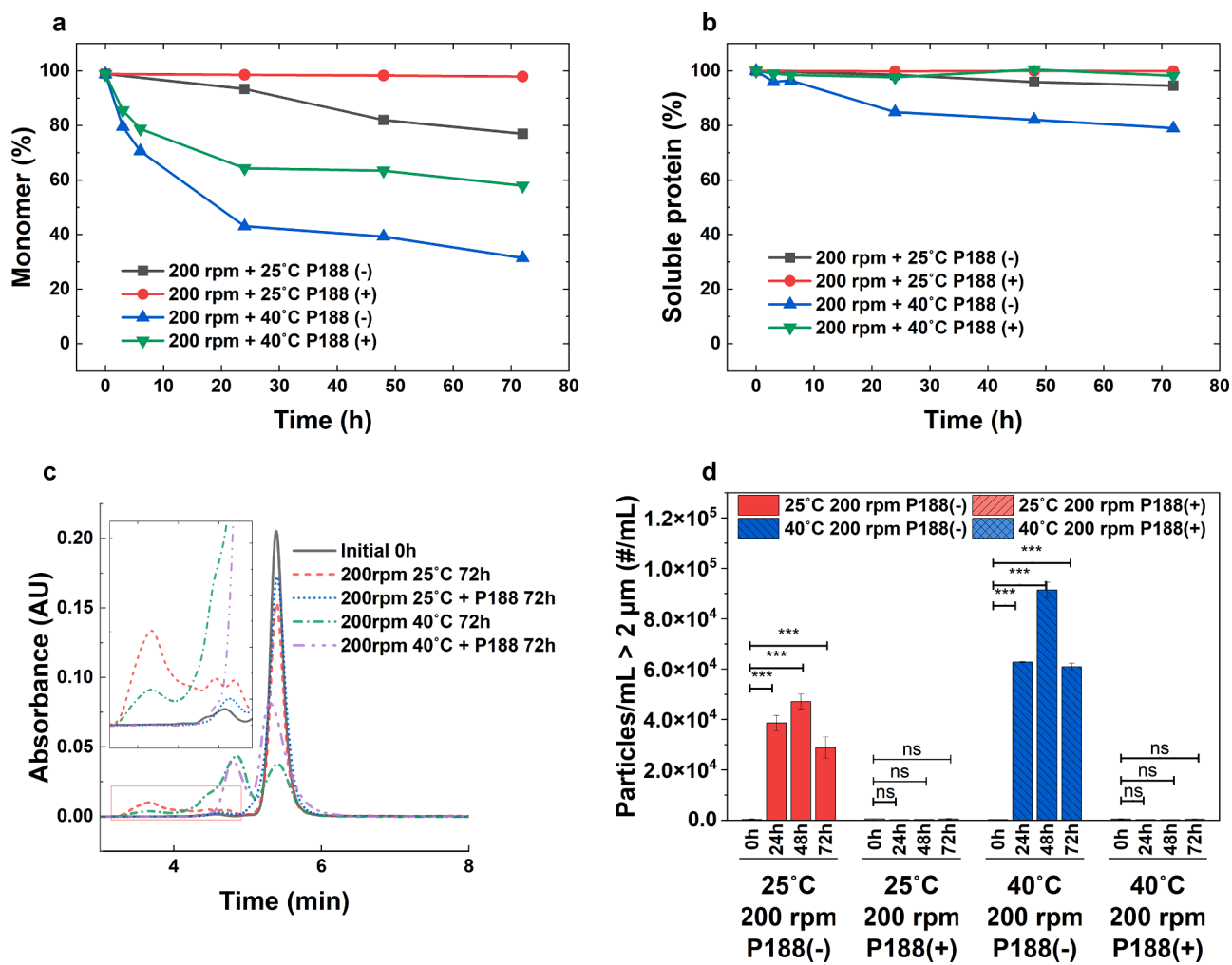


Fig. 4. Effect of combined thermal and agitation stress on the stability of 1.0 mg/mL CTLA4-Ig. (a) Monomer loss, (b) soluble protein loss, (c) corresponding SE-HPLC chromatograms, and (d) average particle count measured by FlowCAM at 25 and 40 °C under 200 rpm agitation, with and without P188.

3.3. Temperature dependence of protein aggregation under agitation stress

To evaluate the impact of thermal stress on the protein aggregation caused by agitation stress, CTLA4-Ig solutions were subjected to agitation at 200 rpm at 25 or 40 °C. The agitation stress at 25 or 40 °C decreased the monomer % value, and a more pronounced decrease was observed at 40 °C than at 25 °C (Fig. 4a, b). The total peak area was also decreased under these stresses, suggesting the generation of insoluble aggregates. This effect was supported by the results of FIM, which showed a significant increase of two to three orders of magnitude in the number of particles of insoluble aggregates at both temperatures (Fig. 4d). Micron-sized particles increased up to 48 h and then decreased between 48 and 72 h. A possible explanation for this decrease is the dissociation of micron-sized particles into submicron aggregates, which fall below the detection range of FIM. Consistent with this, DLS measurements (Figure S2) indicated a continuous increase in submicron aggregates up to 72 h. The size distributions of insoluble aggregates are shown in Figure S3, and the representative images and 2D scatter plots of circularity and intensity are shown in Figures S4 and S5, respectively. Although it is difficult to compare samples agitated at 25 and 40 °C with samples agitated at 5 °C because of the limited number of particles, insoluble aggregates that exhibited fibril-like morphologies were observed in the 25 and 40 °C samples. No clear differences in the size distributions or morphological features were observed between agitation at 25 and 40 °C, suggesting that the aggregation occurred through the same mechanism irrespective of temperature. Considering that an increase in insoluble aggregates was not observed under either thermal or agitation stress alone, these results inferred that there was a synergistic effect of the agitation stress at 25 or 40 °C on the generation of insoluble aggregates.

Although the loss of total soluble protein after agitation at 40 °C for 72 h, as measured by SE-HPLC, was approximately four-fold higher than that at 25 °C, the number of insoluble aggregates generated under the same conditions was only approximately two-fold higher. This discrepancy is likely due to differences in the formation of submicron aggregates, which cannot be detected by SEC or FIM. DLS measurements (Figure S2) indicated that larger submicron aggregates were generated by agitation at 40 °C than at 25 °C.

The elution profile of soluble aggregates was also different between 25 and 40 °C; soluble aggregate peaks were eluted over a wider range at 40 °C (eluted between 3.4 and 5.1 min) than at 25 °C (eluted between 3.4 and 4.8 min) (Fig. 4c). In other words, the elution profile of soluble aggregates at 25 °C looked similar to that under agitation alone (200 rpm at 5 °C), whereas the elution profile of soluble aggregates at 40 °C appeared to include peaks from LEO generated at 40 °C without agitation (eluted at approximately 5 min) (Figure S6).

The addition of 0.8 % P188 effectively suppressed the reduced monomer % observed at 25 °C and partially suppressed that observed at 40 °C (Fig. 4a). Fig. 4c shows that the content of LEO was increased at 40 °C even in the presence of P188, whereas the content of EEO was not. The total peak area, which equates to the amount of soluble protein, was unchanged when 0.8 % P188 was added (Fig. 4b). This result was consistent with the results of FIM (Fig. 4d), which showed no significant increase in insoluble aggregate levels from the initial time points. Therefore, in the presence of P188, monomer loss caused by the agitation stress at 40 °C lead only to the formation of LEO.

The prevention of the generation of insoluble aggregates and EEO by the addition of 0.8 % P188 inferred that these materials may be generated via an interface-mediated pathway (Kiese et al., 2008; Kizuki et al., 2023). This conclusion was corroborated by an experiment that showed that the generation of insoluble aggregates and EEO by the agitation stress at 40 °C could be prevented by eliminating the free air-liquid interface (Figure S7). These findings also suggested that LEO, which were insensitive to P188, could be generated in bulk solution (Li and Roberts, 2010).

3.4. Analysis of the synergistic effects of the temperature on agitation-induced aggregate clusters

The SE of thermal and agitation stresses on LEO, EEO, and insoluble aggregates was evaluated. The SE on LEO (Table 1) and EEO (Table 2) was different: a competitive effect (SE<1) was observed for LEO, and a synergistic effect (SE>1) was observed for EEO. According to the definition of SE, the SE value for insoluble aggregates should be calculated as positive infinity because the content of insoluble aggregates was increased only under the agitation stress at 25 °C or 40 °C.

Regarding the LEO, the SE value of <1 indicated a competitive effect, which means that the agitation stress at 25 °C or 40 °C resulted in smaller amounts of LEO than the sum of the LEO under each stress individually. This result is likely because the LEO were generated in bulk solution at 40 °C; however, interface-mediated aggregation induced by agitation led to further aggregation of LEO at a faster rate than the generation in bulk solution.

A previous study has suggested that the aggregation via interfaces was temperature dependent (Wood et al., 2020). Interface-mediated aggregation occurs through the following steps: diffusion of proteins to the interface; adsorption of proteins; unfolding of proteins; film (aggregate) formation; and desorption and influx of the aggregate into the bulk solution (Bee et al., 2012; Koepf et al., 2018). Because the adsorption and conformation rearrangement steps have an activation energy barrier that can be overcome by thermal energy, a higher temperature results in greater surface activity of proteins (Griffin et al., 2022). The acceleration of the interface-mediated aggregation caused by high temperatures is a possible explanation of the synergistic effect. However, another possibility is that the LEO are precursors of EEO and insoluble aggregates, and the acceleration of the generation of LEO by thermal stress results in a higher amount of EEO and insoluble aggregates.

3.5. Aggregation after pre-heating at 40 °C

To examine the contribution of LEO to the synergistic effect of thermal and agitation stresses, we prepared samples containing a higher amount of LEO by pre-heating the samples at 40 °C and then subjecting the samples to the agitation stress at 25 °C. The pre-incubation at 40 °C increased the amount of LEO by 27 %, whereas pre-incubation at 5 °C did not increase the amount of LEO. The total peak area was not changed by pre-incubation at 5 or 40 °C (Fig. 5a, b).

Agitation stress at 25 °C was applied to the samples containing different amounts of LEO (Fig. 5c, d). Under the agitation stress at 25 °C, the amount of EEO was increased and the total peak area was decreased (denoting the formation of insoluble aggregates) (Fig. 6a, d, e). By contrast, incubation at 25 °C without agitation stress did not increase the amount of EEO or decrease the total peak area (Fig. 5a, b). Thus, there was a combined effect of agitation and thermal stress at 25 °C. Regarding the peak area of the high LEO group, the monomer area was not obviously changed from 24 to 72 h, while the area representing LEO was decreased by approximately 14 % and that for EEO was increased by approximately 17 %, which are almost corresponding levels (Fig. 6b–d). This result indicated that LEO could be converted to EEO by the agitation stress at 25 °C, meaning that LEO are precursors of EEO. Because the generation of EEO and insoluble aggregates is likely to occur at the interface (Fig. 4c), both monomers and LEO have the opportunity to adsorb onto the interface to undergo further aggregation. However, because the area of adsorption sites on the interface is limited (Lu et al., 2016), a higher ratio of LEO can competitively reduce the chance for monomers to adsorb on the interface. This competitive adsorption likely explains why the monomer loss was faster in samples containing less LEO.

Regarding insoluble aggregates, the number of particles captured by FIM increased up to 48 h, followed by a decrease between 48 and 72 h in the sample with a low amount of LEO. This decreasing trend could be

Table 1

Accumulation of late-eluting oligomers (LEO) under thermal stress, and agitation stress with 200 rpm at 5, 25, and 40 °C, and the corresponding synergistic effect values. ($n = 3$).

Temperature (°C)	Time point (h)	OE ^a Thermal (%)	OE _{Agitation} (%)	OE _{Thermal+Agitation} (%)	TE ^b _{Thermal+Agitation} (%)	SE ^c
25 °C	24h	1.23	4.27	2.46	5.45	0.45
	48h	1.38	7.67	4.47	8.94	0.50
	72h	1.36	9.91	5.19	11.14	0.47
40 °C	24h	51.78	4.27	39.61	53.84	0.74
	48h	60.30	7.67	31.32	63.34	0.49
	72h	65.16	9.91	23.33	68.61	0.34

^a OE = observed effect.

^b TE = theoretical effect.

^c SE = synergistic effect.

Table 2

Accumulation of early-eluting oligomers (EEO) under thermal stress, and agitation stress with 200 rpm at 5, 25, and 40 °C, and the corresponding synergistic effect values. ($n = 3$).

Temperature (°C)	Time point (h)	OE ^a Thermal (%)	OE _{Agitation} (%)	OE _{Thermal+Agitation} (%)	TE ^b _{Thermal+Agitation} (%)	SE ^c
25 °C	24h	0.00	4.69	2.71	4.69	0.58
	48h	0.00	5.11	9.44	5.11	1.85
	72h	0.00	6.15	12.46	6.15	2.03
40 °C	24h	0.00	4.69	15.86	4.69	3.38
	48h	0.00	5.11	32.78	5.11	6.42
	72h	0.00	6.15	41.38	6.15	6.73

^a OE = observed effect.

^b TE = theoretical effect.

^c SE = synergistic effect.

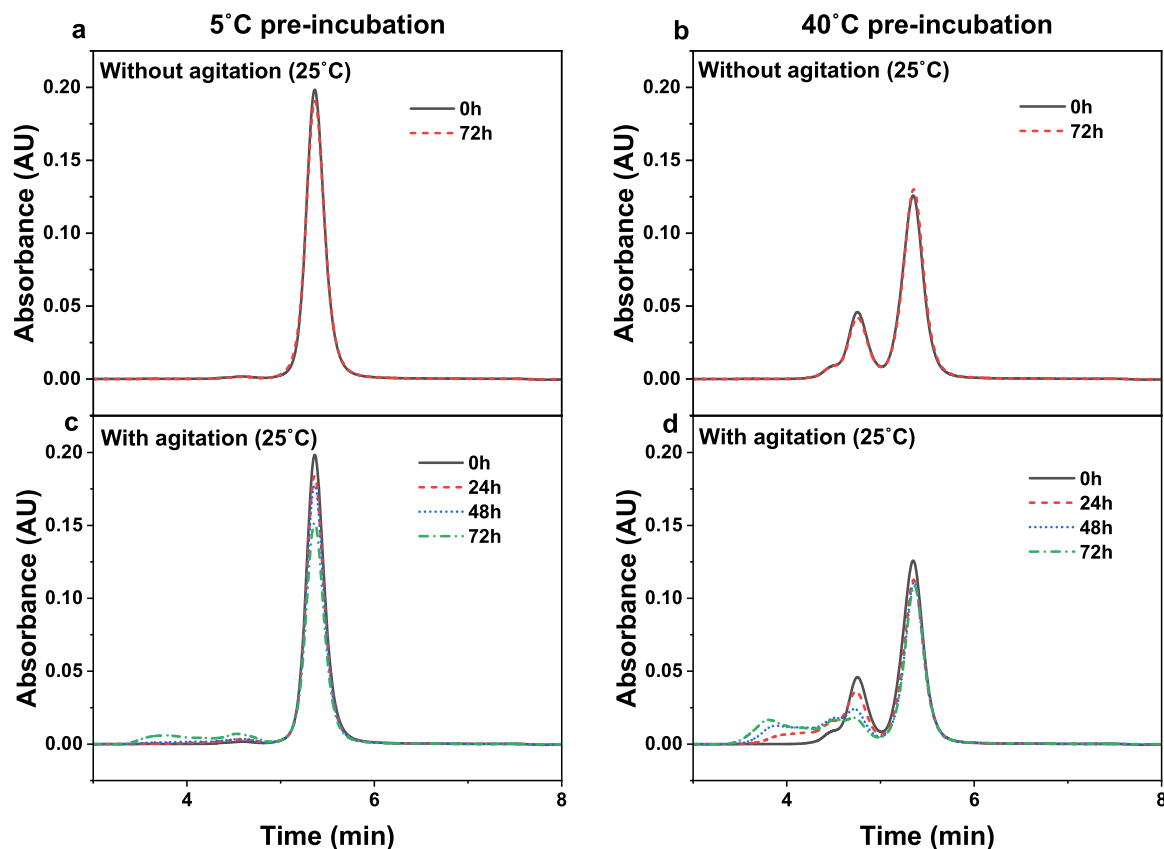


Fig. 5. Preparation of CTLA4-Ig containing a larger amount of LEO. The SE-HPLC chromatograms of CTLA4-Ig after 72-h pre-incubation at (a) 5 °C and (b) 40 °C followed by quiescent standing at 25 °C for another 72 h, and (c, d) after agitation at 200 rpm and 25 °C.

attributed to the dissociation of micron-sized particles into submicron aggregates as with the samples agitated at 200 rpm rotation frequency at both 25 and 40 °C (Fig. 4d). Comparing the results for the samples

containing high and low amounts of LEO, the number of insoluble aggregates in the high LEO group was smaller than that in the low LEO group (Fig. 6e). In addition, the decrease in the monomer % and the total

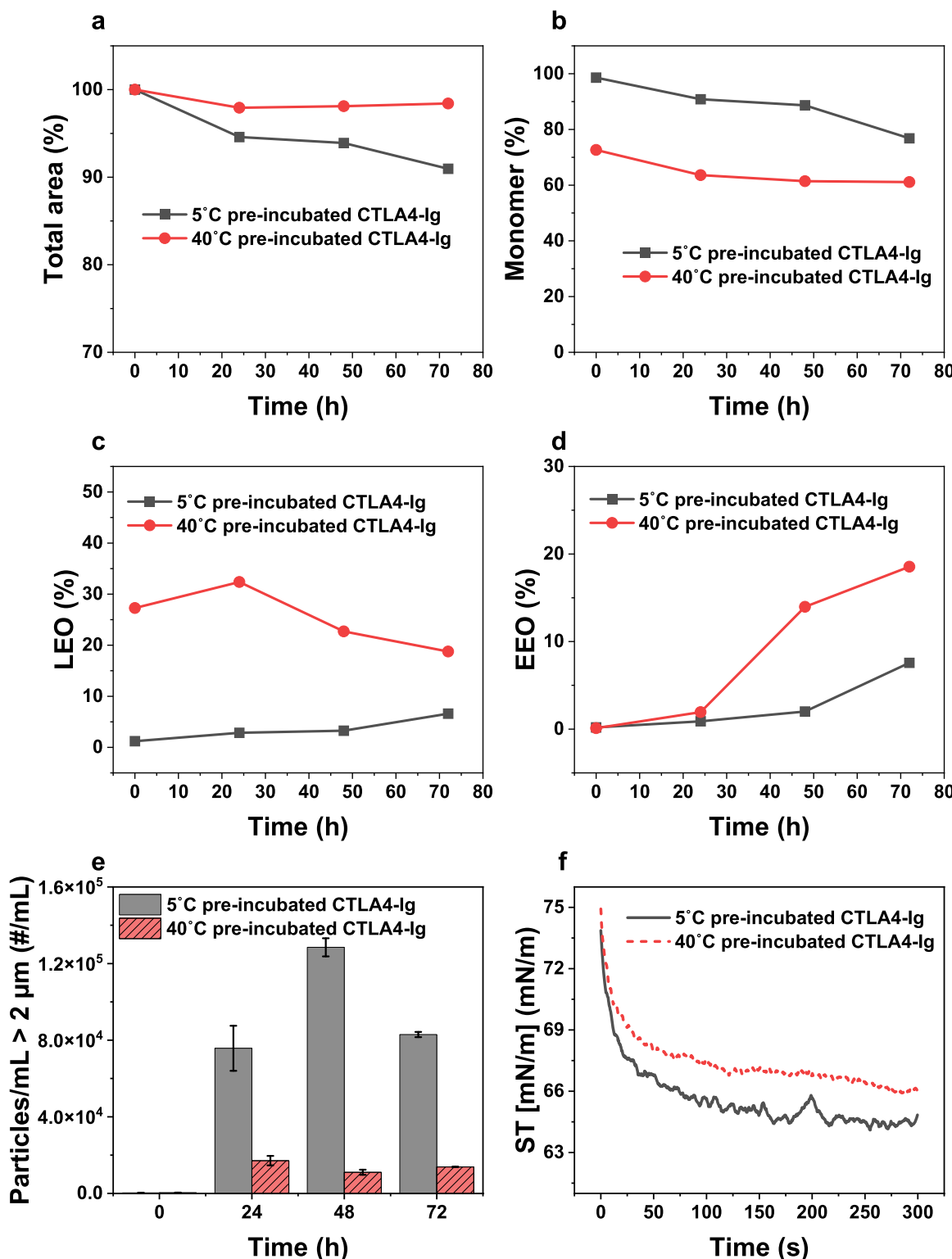


Fig. 6. Stability of CTLA4-Ig after 72 h at 25 °C and 200 rpm agitation after pre-incubation at 5 and 40 °C. (a) Total area of the SE-HPLC chromatogram and relative amounts of (b) monomer, (c) late-eluting oligomers (LEO), and (d) early-eluting oligomers (EEO) as percentages of the total protein. (e) Amount of insoluble aggregates measured by FlowCAM after 200 rpm agitation stability testing at 25 °C. (f) Surface tension of CTLA4-Ig solutions after pre-incubation.

peak area was smaller in the high LEO group.

The monomers were fractionated from the 40 °C pre-incubation sample and analyzed by CD spectroscopy. Although there were subtle differences in the spectra (Figure S8) compared with the 5 °C pre-incubation sample, these differences could be because of some slight amounts of LEO remaining after the fractionation (Figure S9). The

results indicated that the monomer structure did not undergo clear conformational changes upon pre-incubation at 40 °C. Taken together, these results suggest that neither the increased amount of LEO nor a conformational change of the monomer can explain the synergistic increase of insoluble aggregates.

The surface tension with the high LEO group decreased more slowly

than with the low LEO group (Fig. 6f), suggesting slower protein adsorption to the air-liquid interface occurred for samples having a higher ratio of LEO to monomers. Aggregates show slower surface adsorption compared with the monomer because the larger hydrodynamic size results in a slower diffusion rate (Hua et al., 2021). Given that EEO and insoluble aggregates were generated via an interface-mediated route, the increase in LEO, which have a slower adsorption rate, might be unfavorable to increase the amounts of EEO and insoluble aggregates. Nevertheless, a synergistic effect on the generation of EEO and insoluble aggregates was observed. Therefore, acceleration of the formation of LEO could not be the cause of the synergistic effect.

3.6. Agitation threshold for aggregate formation

The influence of high temperatures on the threshold of the agitation conditions that caused an increase in EEO and insoluble aggregates was evaluated. Five different agitation frequencies (0, 100, 150, 180, and 200 rpm) were applied at three temperatures (5, 25, and 40 °C) (Fig. 7). An increase or decrease of 2 % in the area % value was used as the criteria for observable changes, balancing the precision of SEC measurements with the interference of minor fluctuations.

The threshold of the aggregation frequency that induced aggregation was determined primarily based on the decrease in the monomer % value. At 5 and 25 °C, a clear decrease in the monomer content was observed at agitation frequencies of 180 and 200 rpm (Fig. 7a), suggesting the rotation frequency threshold was between 150 and 180 rpm. Because the decrease in the monomer % at 40 °C also resulted from the generation of LEO, the threshold was determined to be between 150 and 180 rpm based on the increase in EEO and insoluble aggregates (Fig. 7b, c). Thus, the threshold of the agitation frequency that induced aggregation may be independent of the temperature. In the present study, the threshold was defined as the boundary between conditions where the aggregates increased and conditions where the aggregates did not increase, irrespective of aggregate clusters. Because agitation-induced aggregates were still observed even at 5 °C, no temperature threshold was considered to be present for CTLA4-Ig under the current conditions. However, elevated temperatures, especially temperatures above the T_{onset} value, could induce structural changes leading to the formation of distinct aggregate clusters under agitation.

Although the temperature did not affect the threshold of the agitation frequency that induced aggregation, the aggregate clusters of EEO and insoluble aggregates were affected by the temperature. When the result at 180 rpm was compared with that at 200 rpm, the EEO % was larger when the insoluble aggregates % was smaller (Fig. 7b, c). More specifically, a higher rotation frequency resulted in a higher amount of insoluble aggregates and a lower amount of EEO. The size of aggregates

induced by agitation can be determined by the kinetics of the adsorption to the air-liquid interface and subsequent unfolding and aggregation of the proteins at the interface. Higher temperatures can accelerate the adsorption by enhancing molecular kinetic energy, unfolding, and aggregation of proteins at the air-liquid interface. The rotation frequency also affects protein aggregation at the air-liquid interface (Johann et al., 2022). Consequently, the aggregate clusters also depended on the temperature and rotation frequency. The threshold of the agitation frequency that increases aggregate formation may be related to the release of aggregates from the interface, which could be less affected by temperature than other factors (Schwartz et al., 2023). Although the present study provides valuable insights into the temperature-dependence of the agitation-induced aggregation of CTLA4-Ig, it should be noted that different proteins have different conformational and interfacial stability, and further studies are needed to investigate a wider range of proteins, such as IgG, to draw a more general conclusion.

3.7. Stability studies of agitation stress under controlled temperatures

Interfacial stress is widely recognized as a cause of protein aggregation. Our recent study showed the usefulness of including a shaking stress study in formulation development (Okada et al., 2025). A previous survey has shown that stress stability studies using a shaker are often conducted during the development of biopharmaceuticals, and that the temperature is not controlled in most of these shaking stress studies (Halley et al., 2020). Meng et al. have demonstrated that a combination of thermal and pH stress can offer a more holistic evaluation of aggregation propensity and may improve the efficiency of developability assessments (Meng et al., 2024). Below, the value of agitation stress at 25 °C or 40 °C in the development of biopharmaceuticals is discussed.

Temperature control during agitation stress testing is important to ensure reproducibility because the amounts and aggregate clusters are temperature dependent. In addition, when the stability under a certain condition is evaluated, the expected temperature should be used. For instance, the temperature should be set to the room temperature of the hospital when the agitation stresses during handling in the hospital are to be evaluated. When the impact of agitation during storage or transport at 5 °C is evaluated, the agitation stress studies should be conducted at 5 °C.

As shown in the present study, a combination stress study using a high temperature and agitation can provide information on the degradation caused by each stress (high temperature and agitation) simultaneously, leading to more efficient development. These findings highlight the value of the agitation stress study at 40 °C to provide deep insights into aggregation caused by accidental exposure (e.g., during transportation) and in evaluating test parameters for monitoring product

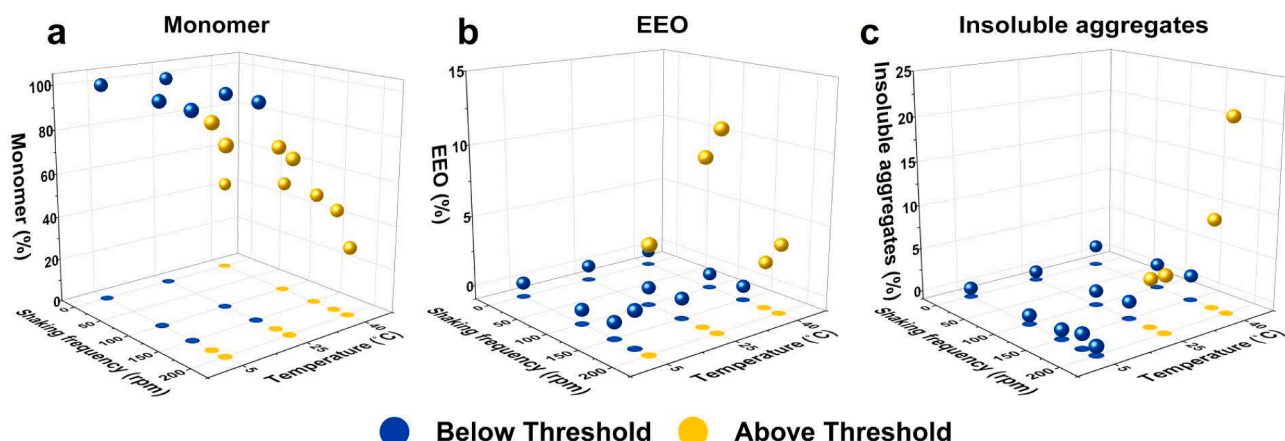


Fig. 7. Rotation frequency threshold for the formation of aggregates in 1.0 mg/mL CTLA4-Ig under different temperatures. (a) Monomer, (b) early-eluting oligomers (EEO), and (c) insoluble aggregates.

stability. Therefore, a temperature of 40 °C is also a valuable condition for stability evaluation, although such conditions rarely occur in real-world situations (Sreenivasan et al., 2024). Strebl et al. have suggested that different proteins may exhibit different aggregation mechanisms even under the same thermal conditions (Strebl et al., 2024), and thus investigating the stability of proteins other than CTLA4-Ig under agitation stress at 25 °C or 40 °C in future studies will provide critical information to design a sophisticated stability study approach.

In addition to high temperatures, freezing is another stress that can affect agitation-induced aggregation. Although the frozen state is generally effective in mitigating aggregation caused by agitation stress, pH shifts during freezing, particularly in phosphate buffers (Thorat et al., 2020), can lead to structural changes and thereby increase aggregation after thawing. The combined effect of freeze/thaw and agitation stresses will be investigated in our future work.

4. Conclusions

Protein aggregation is difficult to prevent completely, and thus the analysis and control of protein aggregates are required. Understanding the temperature dependence of agitation-induced aggregation is important, not only for preventing aggregation caused by the combination of agitation and thermal stress that can occur during shipping, but also for designing better agitation stress studies. The present study elucidated the mechanistic interactions between combined thermal and agitation stresses in the formation of aggregates of CTLA4-Ig. The levels of EEO and insoluble aggregates formed by agitation stress were temperature dependent and were synergistically accelerated by thermal stress. In addition, the formation of aggregate clusters was temperature dependent. These results could be because high temperatures increase the surface activity and affect protein unfolding and aggregate formation at the air-liquid interface. By contrast, the threshold of shaking conditions for the formation of EEO and insoluble aggregates was temperature independent, indicating that the release of aggregates from the air-liquid interface was less sensitive to temperature. These results clearly show the importance of controlling the temperature under situations, such as in shipping, during which proteins are exposed to agitation and thermal stress at the same time. The temperature should also be controlled carefully during shaking stress studies to ensure reproducibility. Shaking stress studies at elevated temperatures can be used to either represent real-world stress conditions or function as a forced degradation method to contribute to formulation development.

Funding

The present study was partly supported by JSPS KAKENHI Grant Number 24K18261 to TT. This work was supported by JST, the establishment of university fellowships towards the creation of science technology innovation, Grant Number JPMJFS2125.

CRediT authorship contribution statement

Zekun Wang: Writing – review & editing, Writing – original draft, Investigation, Data curation. **Arni Gambe-Gilbuena:** Investigation. **Satoru Unzai:** Investigation. **Susumu Uchiyama:** Writing – review & editing, Supervision. **Tetsuo Torisu:** Writing – review & editing, Writing – original draft, Supervision, Conceptualization.

Declaration of competing interest

The authors declare that they have no known competing financial interests or personal relationships that could have appeared to influence the work reported in this paper.

Acknowledgement

The authors thank Victoria Muir, PhD, from Edanz (<https://jp.edanz.com/ac>) for editing the English text of a draft of this manuscript.

Supplementary materials

Supplementary material associated with this article can be found, in the online version, at [doi:10.1016/j.ejps.2025.107320](https://doi.org/10.1016/j.ejps.2025.107320).

Data availability

Data will be made available on request.

References

Amin, S., Barnett, G.V., Pathak, J.A., Roberts, C.J., Sarangapani, P.S., 2014. Protein aggregation, particle formation, characterization & rheology. *Curr. Opin. Colloid Interface Sci.* 19, 438–449. <https://doi.org/10.1016/j.cocis.2014.10.002>.

Anthis, N.J., Clore, G.M., 2013. Sequence-specific determination of protein and peptide concentrations by absorbance at 205 nm. *Protein Sci.* 22, 851–858. <https://doi.org/10.1002/pro.2253>.

Arsiccio, A., Pisano, R., 2018. Surfactants as stabilizers for biopharmaceuticals: an insight into the molecular mechanisms for inhibition of protein aggregation. *Europ. J. Pharmaceut. Biopharmaceut.* 128, 98–106. <https://doi.org/10.1016/j.ejpb.2018.04.005>.

Bee, J.S., Schwartz, D.K., Trabelsi, S., Freund, E., Stevenson, J.L., Carpenter, J.F., Randolph, T.W., 2012. Production of particles of therapeutic proteins at the air–water interface during compression/dilation cycles. *Soft. Matter.* 8, 10329. <https://doi.org/10.1039/c2sm26184g>.

Bollenbach, L., Buske, J., Mäder, K., Garidel, P., 2022. Poloxamer 188 as surfactant in biological formulations – An alternative for polysorbate 20/80? *Int. J. Pharm.* 620, 121706. <https://doi.org/10.1016/j.ijpharm.2022.121706>.

Cappelletto, E., Kwok, S.C., Sorret, L., Fuentes, N., Medina, A.M., Burleigh, S., Fast, J., Mackenzie, I.S., Fireby, A.M., Paulsson, M., Wahlgren, M., Elofsson, U., Flynn, A., Miolo, G., Nyström, L., De Laureto, P.P., De Paoli, G., 2024. Impact of post manufacturing handling of protein-based biologic drugs on product quality and user centricity. *J. Pharm. Sci.* 113, 2055–2064. <https://doi.org/10.1016/j.xphs.2024.05.027>.

Carpenter, J.F., Randolph, T.W., Jiskoot, W., Crommelin, D.J.A., Russell Middaugh, C., Winter, G., Fan, Y.-X., Kirshner, S., Verhelyi, D., Kozlowski, S., Clouse, K.A., Swann, P.G., Rosenberg, A., Cherney, B., 2009. Overlooking subvisible particles in therapeutic protein products: gaps that may compromise product quality. *J. Pharm. Sci.* 98, 1201–1205. <https://doi.org/10.1002/jps.21530>.

Czajkowski, D.M., Hu, J., Shao, Z., Pless, R.J., 2012. Fc-fusion proteins: new developments and future perspectives. *EMBO Mol. Med.* 4, 1015–1028. <https://doi.org/10.1002/emmm.201201379>.

Das, T.K., Narhi, L.O., Sreedhara, A., Menzen, T., Grapentin, C., Chou, D.K., Antochchuk, V., Filipe, V., 2020. Stress factors in mAb drug substance production processes: critical assessment of impact on product quality and control strategy. *J. Pharm. Sci.* 109, 116–133. <https://doi.org/10.1016/j.xphs.2019.09.023>.

Fast, J.L., Cordes, A.A., Carpenter, J.F., Randolph, T.W., 2009. Physical instability of a therapeutic fc fusion protein: domain contributions to conformational and colloidal stability. *Biochemistry* 48, 11724–11736. <https://doi.org/10.1021/bi900853v>.

Fathallah, A.M., Chiang, M., Mishra, A., Kumar, S., Xue, L., Russell Middaugh, C., Balu-Iyer, S.V., 2015. The effect of small oligomeric protein aggregates on the immunogenicity of intravenous and subcutaneous administered antibodies. *J. Pharm. Sci.* 104, 3691–3702. <https://doi.org/10.1002/jps.24592>.

Freitag, A.J., Shomali, M., Michalakis, S., Biel, M., Siedler, M., Kaymakcalan, Z., Carpenter, J.F., Randolph, T.W., Winter, G., Engert, J., 2015. Investigation of the immunogenicity of different types of aggregates of a murine monoclonal antibody in mice. *Pharm. Res.* 32, 430–444. <https://doi.org/10.1007/s11095-014-1472-6>.

Ghazvini, S., Kalonia, C., Volkin, D.B., Dhar, P., 2016. Evaluating the role of the air–solution interface on the mechanism of subvisible particle formation caused by mechanical agitation for an IgG1 mAb. *J. Pharm. Sci.* 105, 1643–1656. <https://doi.org/10.1016/j.xphs.2016.02.027>.

González, E.A., Nazareno, M.A., 2011. Antiradical action of flavonoid–ascorbate mixtures. *LWT - Food Sci. Technol.* 44, 558–564. <https://doi.org/10.1016/j.lwt.2010.09.017>.

Griffin, V.P., Merritt, K., Vaclav, C., Whitaker, N., Volkin, D.B., Ogunyankin, M.O., Pace, S., Dhar, P., 2022. Evaluating the combined impact of temperature and application of interfacial dilatational stresses on surface-mediated protein particle formation in monoclonal antibody formulations. *J. Pharm. Sci.* 111, 680–689. <https://doi.org/10.1016/j.xphs.2021.10.038>.

Grigolato, F., Arosio, P., 2020. Synergistic effects of flow and interfaces on antibody aggregation. *Biotechnol. Bioeng.* 117, 417–428. <https://doi.org/10.1002/bit.27212>.

Grilo, A.L., Mantalaris, A., 2019. The increasingly Human and profitable monoclonal antibody market. *Trends Biotechnol.* 37, 9–16. <https://doi.org/10.1016/j.tibtech.2018.05.014>.

Halley, J., Chou, Y.R., Cicchino, C., Huang, M., Sharma, V., Tan, N.C., Thakkar, S., Zhou, L.L., Al-Azzam, W., Cornen, S., Gauden, M., Gu, Z., Kar, S., Lazar, A.C.,

Mehndiratta, P., Smith, J., Sosic, Z., Weisbach, P., Stokes, E.S.E., 2020. An industry perspective on forced degradation studies of biopharmaceuticals: survey outcome and recommendations. *J. Pharm. Sci.* 109, 6–21. <https://doi.org/10.1016/j.xphs.2019.09.018>.

Hua, X., Liu, J., Guan, S., Tan, J., Wang, M., Yang, R., 2021. Surface activity of ultrahigh methoxylated pectin of different size. *Food Hydrocoll.* 113, 106495. <https://doi.org/10.1016/j.foodhyd.2020.106495>.

Johann, F., Wöll, S., Winzer, M., Snell, J., Valldorf, B., Gieseler, H., 2022. Miniaturized forced degradation of therapeutic proteins and ADCs by agitation-induced aggregation using orbital shaking of microplates. *J. Pharm. Sci.* 111, 1401–1413. <https://doi.org/10.1016/j.xphs.2021.09.027>.

Kiese, S., Pappenberg, A., Friess, W., Mahler, H.-C., 2008. Shaken, not stirred: mechanical stress testing of an IgG1 antibody. *J. Pharm. Sci.* 97, 4347–4366. <https://doi.org/10.1002/jps.21328>.

Kijanka, G., Bee, J.S., Korman, S.A., Wu, Y., Roskos, L.K., Schennerman, M.A., Slüter, B., Jiskoot, W., 2018. Submicron size particles of a murine monoclonal antibody are more immunogenic than soluble oligomers or micron size particles upon subcutaneous administration in mice. *J. Pharm. Sci.* 107, 2847–2859. <https://doi.org/10.1016/j.xphs.2018.06.029>.

Kizuki, S., Wang, Z., Torisu, T., Yamauchi, S., Uchiyama, S., 2023. Relationship between aggregation of therapeutic proteins and agitation parameters: acceleration and frequency. *J. Pharm. Sci.* 112, 492–505. <https://doi.org/10.1016/j.xphs.2022.09.022>.

Kizuki, S., Wang, Z., Yamauchi, S., Torisu, T., Uchiyama, S., 2025. Impact of weak vibration generated by a refrigerator on protein aggregation. *AAPS J.* 27, 34. <https://doi.org/10.1208/s12248-025-01014-z>.

Koepf, E., Eisele, S., Schroeder, R., Brezesinski, G., Friess, W., 2018. Notorious but not understood: how liquid-air interfacial stress triggers protein aggregation. *Int. J. Pharm.* 537, 202–212. <https://doi.org/10.1016/j.ijpharm.2017.12.043>.

Krayukhina, E., Yokoyama, M., Hayashihara, K.K., Maruno, T., Noda, M., Watanabe, H., Uchihashi, T., Uchiyama, S., 2019. An assessment of the ability of submicron- and micron-size silicone oil droplets in dropped preffillable syringes to invoke early- and late-stage immune responses. *J. Pharm. Sci.* 108, 2278–2287. <https://doi.org/10.1016/j.xphs.2019.02.002>.

Li, J., Krause, M.E., Chen, X., Cheng, Y., Dai, W., Hill, J.J., Huang, M., Jordan, S., LaCasse, D., Narhi, L., Shalaev, E., Shieh, I.C., Thomas, J.C., Tu, R., Zheng, S., Zhu, L., 2019. Interfacial stress in the development of biologics: fundamental understanding, current practice, and future perspective. *AAPS J.* 21, 44. <https://doi.org/10.1208/s12248-019-0312-3>.

Li, J., Zeng, C., Guan, J., Suryanarayanan, R., 2024. Effect of surfactants on lactate dehydrogenase aqueous solutions: a comparative study of poloxamer 188, polysorbate 20 and 80. *Int. J. Pharm.* 661, 124374. <https://doi.org/10.1016/j.ijpharm.2024.124374>.

Li, Y., Roberts, C.J., 2010. Protein aggregation pathways, kinetics, and thermodynamics. *Aggregat. Therapeut. Proteins.* Wiley 63–102. <https://doi.org/10.1002/9780470769829.ch2>.

Lu, Q., Tang, Q., Xiong, Y., Qing, G., Sun, T., 2016. Protein/Peptide Aggregation and Amyloidosis on Biointerfaces. *Materials* 9, 740. <https://doi.org/10.3390/ma9090740>.

Meng, H.K., Pang, K.T., Wan, C., Zheng, Z.Y., Beiyiing, Q., Yang, Y., Zhang, W., Ho, Y.S., Walsh, I., Chia, S., 2024. Thermal and pH stress dictate distinct mechanisms of monoclonal antibody aggregation. *Int. J. Biol. Macromol.* 282, 136601. <https://doi.org/10.1016/j.ijbiomac.2024.136601>.

Moussa, E.M., Panchal, J.P., Moorthy, B.S., Blum, J.S., Joubert, M.K., Narhi, L.O., Topp, E.M., 2016. Immunogenicity of therapeutic protein aggregates. *J. Pharm. Sci.* 105, 417–430. <https://doi.org/10.1016/j.xphs.2015.11.002>.

Okada, R., Shibata, K., Shibuya, R., Torisu, T., Uchiyama, S., 2025. Hierarchical clustering of therapeutic proteins based on agitation-induced aggregation propensity and its relation to physicochemical parameters. *Europ. J. Pharmaceut. Sci.* 208, 107060. <https://doi.org/10.1016/j.ejps.2025.107060>.

Roberts, C.J., Das, T.K., Sahin, E., 2011. Predicting solution aggregation rates for therapeutic proteins: approaches and challenges. *Int. J. Pharm.* 418, 318–333. <https://doi.org/10.1016/j.ijpharm.2011.03.064>.

Rosenberg, A.S., 2006. Effects of protein aggregates: an immunologic perspective. *AAPS J.* 8, E501–E507. <https://doi.org/10.1208/aapsj080359>.

Schvartz, M., Saudrais, F., Devineau, S., Aude, J.-C., Chédin, S., Henry, C., Millán-Oropeza, A., Perrault, T., Pieri, L., Pin, S., Boulard, Y., Brotons, G., Renault, J.-P., 2023. A proteome scale study reveals how plastic surfaces and agitation promote protein aggregation. *Sci. Rep.* 13, 1227. <https://doi.org/10.1038/s41598-023-28412-7>.

Scomorocenco, C., Teodorescu, M., Burlacu, S.G., Gîfu, I.C., Mihaescu, C.I., Petcu, C., Raducan, A., Oancea, P., Cîntea, L.O., 2022. Synergistic antioxidant activity and enhanced stability of curcumin encapsulated in vegetal oil-based microemulsion and gel microemulsions. *Antioxidants* 11, 854. <https://doi.org/10.3390/antiox11050854>.

Sperinde, G., Montgomery, D., Mytych, D.T., 2020. Clinical immunogenicity risk assessment for a fusion protein. *AAPS J.* 22, 64. <https://doi.org/10.1208/s12248-020-00447-y>.

Sreenivasan, S., Jiskoot, W., Rathore, A.S., 2021a. Rapid aggregation of therapeutic monoclonal antibodies by bubbling induced air/liquid interfacial and agitation stress at different conditions. *Europ. J. Pharmaceut. Biopharmaceut.* 168, 97–109. <https://doi.org/10.1016/j.ejpb.2021.08.010>.

Sreenivasan, S., Schöneich, C., Rathore, A.S., 2024. Aggregation of therapeutic monoclonal antibodies due to thermal and air/liquid interfacial agitation stress: occurrence, stability assessment strategies, aggregation mechanism, influencing factors, and ways to enhance stability. *Int. J. Pharm.* 666, 124735. <https://doi.org/10.1016/j.ijpharm.2024.124735>.

Sreenivasan, S., Sonawat, D., Mandal, S., Khare, K., Rathore, A.S., 2021b. Novel semi-automated fluorescence microscope imaging algorithm for monitoring IgG aggregates in serum. *Sci. Rep.* 11, 11375. <https://doi.org/10.1038/s41598-021-90623-7>.

Strand, J., Huang, C.-T., Xu, J., 2013. Characterization of Fc-fusion protein aggregates derived from extracellular domain disulfide bond rearrangements. *J. Pharm. Sci.* 102, 441–453. <https://doi.org/10.1002/jps.23421>.

Strebl, M., Arache, A., Blech, M., Bakowsky, U., Garidel, P., 2024. Evaluating the influence of the initial high molecular weight level on monoclonal antibody particle formation kinetics using a short-term chemical stress study. *Europ. J. Pharmaceut. Sci.* 203, 106924. <https://doi.org/10.1016/j.ejps.2024.106924>.

Telikepalli, S., Shinogle, H.E., Thapa, P.S., Kim, J.H., Deshpande, M., Jawa, V., Russell Middaugh, C., Narhi, L.O., Joubert, M.K., Volkin, D.B., 2015. Physical characterization and *In vitro* biological impact of highly aggregated antibodies separated into size-enriched populations by fluorescence-activated cell sorting. *J. Pharm. Sci.* 104, 1575–1591. <https://doi.org/10.1002/jps.24379>.

Thorat, A.A., Munjal, B., Geders, T.W., Suryanarayanan, R., 2020. Freezing-induced protein aggregation - role of pH shift and potential mitigation strategies. *J. Controlled Release* 323, 591–599. <https://doi.org/10.1016/j.jconrel.2020.04.033>.

Toprakcioglu, Z., Kamada, A., Michaels, T.C.T., Xie, M., Krausser, J., Wei, J., Saric, A., Vendruscolo, M., Knowles, T.P.J., 2022. Adsorption free energy predicts amyloid protein nucleation rates. *Procceed. Nation. Acad. Sci.* 119. <https://doi.org/10.1073/pnas.2109718119>.

Torisu, T., Maruno, T., Hamaji, Y., Ohkubo, T., Uchiyama, S., 2017. Synergistic effect of cavitation and agitation on protein aggregation. *J. Pharm. Sci.* 106, 521–529. <https://doi.org/10.1016/j.xphs.2016.10.015>.

Walsh, G., 2018. Biopharmaceutical benchmarks 2018. *Nat. Biotechnol.* 36, 1136–1145. <https://doi.org/10.1038/nbt.4305>.

Wiesbauer, J., Prassl, R., Nidetzky, B., 2013. Renewal of the air–Water interface as a critical system parameter of protein stability: aggregation of the Human growth hormone and its prevention by surface-active compounds. *Langmuir* 29, 15240–15250. <https://doi.org/10.1021/la4028223>.

Wood, C.V., McEvoy, S., Razinkov, V.I., Qi, W., Furst, E.M., Roberts, C.J., 2020. Kinetics and competing mechanisms of antibody aggregation via bulk- and surface-mediated pathways. *J. Pharm. Sci.* 109, 1449–1459. <https://doi.org/10.1016/j.xphs.2020.01.005>.

Yanwinitchai, S., Dao, H.M., Moon, C., Williams III, R.O., 2024. Synergistic cryoprotective effect of deaeration and polysorbate 80 on IgG denaturation during thin-film freeze-drying. *J. Drug Deliv. Sci. Technol.* 100, 106106. <https://doi.org/10.1016/j.jddst.2024.106106>.

Yoneda, S., Maruno, T., Mori, A., Hioki, A., Nishiumi, H., Okada, R., Murakami, M., Zekun, W., Fukuhara, A., Itagaki, N., Harauchi, Y., Adachi, S., Okuyama, K., Sawaguchi, T., Torisu, T., Uchiyama, S., 2021. Influence of protein adsorption on aggregation in prefilled syringes. *J. Pharm. Sci.* 110, 3568–3579. <https://doi.org/10.1016/j.xphs.2021.07.007>.